Whispering-gallery-mode barcode-based broadband sub-femtometer-resolution spectroscopy with an electro-optic frequency comb: supplemental document

BINGXIN XU[1, 2, †], YANGYANG WAN[1, †], XINYU FAN[1, *], AND ZUYUAN HE[1]

[1] *State Key Laboratory of Advanced Optical Communication Systems and Networks, Shanghai Jiao Tong University, 800 Dongchuan Road, Minhang, Shanghai 200240, China*

[2] *Current Address: Max-Planck Institute of Quantum Optics, Hans-Kopfermann-Straße 1, 85748, Garching, Germany*

* *Corresponding author: fan.xinyu@sjtu.edu.cn*

† *These authors contributed equally to this work*

1. Detailed performance comparison

We compare the proposed system with other works in terms of resolution, bandwidth, stability, refresh rate and complexity/cost effectiveness.

Resolution and bandwidth:
Generally, reconstructive spectrometers (Ref[5,6,17,18]), including speckle-based spectrometers and fs comb-based spectrometer (Ref[25,26]), can achieve pm resolution and over tens of nanometer bandwidth, although some reconstructive spectrometers independently demonstrate resolution and bandwidth. For speckle-based system, higher resolution is limited to determining single or few wavelengths instead of full spectrum, as a wavemeter (Ref[7,8,10,11,12]). For fs comb-based spectrometers, shifting two mutually coherent comb sources locked to atom clock at fine steps can interleave spectrum to fm resolution (Ref[27]) or possibly even higher, which is complicated and may only be performed in advanced metrology laboratory. In contrast, EOFC with freely selected repetition rate, is easier to reach fm and sub-fm resolution (Ref[32-34]), However, its bandwidth is limited, normally proportional to the repetition rate. For fm resolution comb, cascaded EOFC extends the bandwidth with a factor of 20. (Ref[40]). The proposed method combining EOFC and WGM speckle provides 8 fm spectral resolution with 80 nm bandwidth, comparable to interleaved fs-comb based DCS. Remarkably, another demonstration of 0.8 fm resolution by the proposed scheme overperforms existing methods in bandwidth.

Stability:
Long term stability is considerable in all speckle-based system. However, there is no unified stability evaluation index, and low-resolution system has a better long-term stability. Therefore, stability is not included in the Fig. 9. As an exemplified comparison, integrating sphere based wavemeter with sub-femtometer resolution has a measurement offset error of 1.5 pm (about 740 MHz) per hour (Ref[12]). In contrast, the maximum offset within 10 hours in the proposed system is only 400 fm (about 50 MHz), while this offset is eliminated with the scheme of stabilized laser calibration in measurement. Hence no measurement error is introduced, as discussed in the section “4 Long-term

stability", which illustrate a better long-term stability.

Refresh time:

The refresh rates of all displayed schemes are relatively high without mechanism scanning. The refresh time of reconstructive spectrometers is not specified but generally in ms level determined by the exposure time of camera. The refresh rate of DCS and EOFC-based system is related to the pulse repetition rate in kHz level including the proposed method.

Complexity and cost effectiveness.

The complexity and cost-effectiveness of the proposed method with EO-comb and WGM speckle is comparable to existing EO-comb based systems, which is much lower than mutually coherent fs-comb DCS (Ref. [26,27]).

2. Ultra-fine electro-optic frequency generation with tailored waveform

Tailored waveform in electro-optic modulation, instead of overdriving modulator with high-voltage signal, can cost-effectively generate more comb lines, especially for ultra-fine repetition rate. Here, the tailored waveform is the inverse Fourier transformation of multiple frequencies in parabolic phase relation, which looks like chirped pulse in time domain. The waveform can be expressed as

$$E(t) = \sum_{i=1}^{N} \cos\left(2\pi(f_0 + i f_{rep})\,t + \frac{\pi(i-\frac{N}{2})^2}{N}\right) \tag{1}$$

where f_0 is the starting frequency (usually is 0), f_{rep} is the repetition frequency, and N is the number of frequency components. Figure S1 exemplifies a case of N=50. The f_{rep}, N and f_0 are freely selected for any kinds of design. Compared with pulse waveform in zero/linear phase relation, the parabolic-phase waveform better utilizes the limited output vertical range of arbitrary waveform generator and linear amplifier, which is especially significate for the generation of more than ten thousand of comb lines. In our experiments, we respectively use f_{rep}=100 kHz, f_0=0, N=14000, and f_{rep}=1 MHz, f_0=0, N=1450 for comb generation. Waveforms, stored in the memory of arbitrary waveform generator, are easily loaded and changed by clicking a button. A Mach-Zehnder modulator, driven by the tailored waveform, is used for electro-optic comb generation. Totally 2N+1 comb lines, all are first order positive and negative sidebands without phase noise accumulation, are generated.

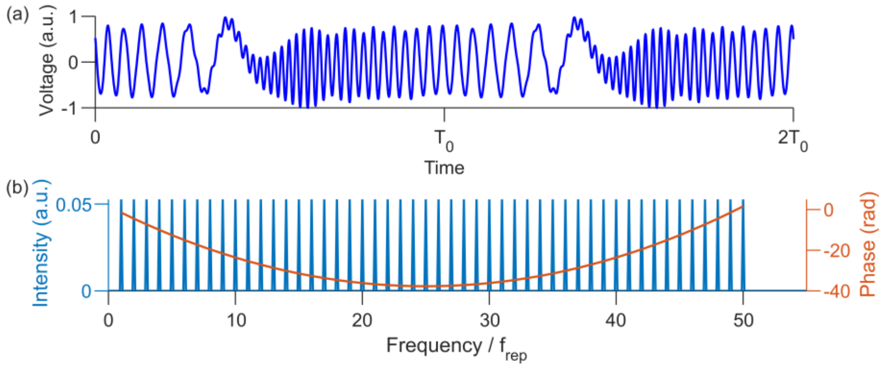

Figure S1 (a) Temporal waveform, (b) intensity spectrum and phase spectrum of the tailored signal for ultra-fine electro-optic modulation with 50 frequency components.

3. Interferograms and radio-frequency spectra of heterodyne interferometer

The electro-optic comb, with 100 kHz or 1 MHz repetition rate, beats with the frequency shifted continuous-wave oscillation in a heterodyne interferometer. Detected by a balanced photo-detector with 1.6-GHz bandwidth and digitized by a data acquisition board with a sample rate of 3.125 GSample/s, the interferograms are shown in Fig. S2(a) and S3(a). The radio frequency spectra, obtained by digital fast Fourier transformation of respectively 1 ms and 100 µs recording, are displayed in Fig. S2(b) and S3(b). The comb lines in about 3-GHz optical bandwidth are folded into 1.5 GHz radio frequency bandwidth. The roll-off of detector response can be observed. Comb lines at high radio frequency (typically larger than 1.25 GHz) with low signal-to-noise ratio are manually removed. The center shifts, introduced by the acoustic-optic modulator are respectively 80.025 MHz and 80.25 MHz with a remainder of a quarter of repetition rate. The comb spectra symmetrically in optical domain are obtained by unfolding the RF spectra, as shown in main text Fig. 4(a) in linear scale.

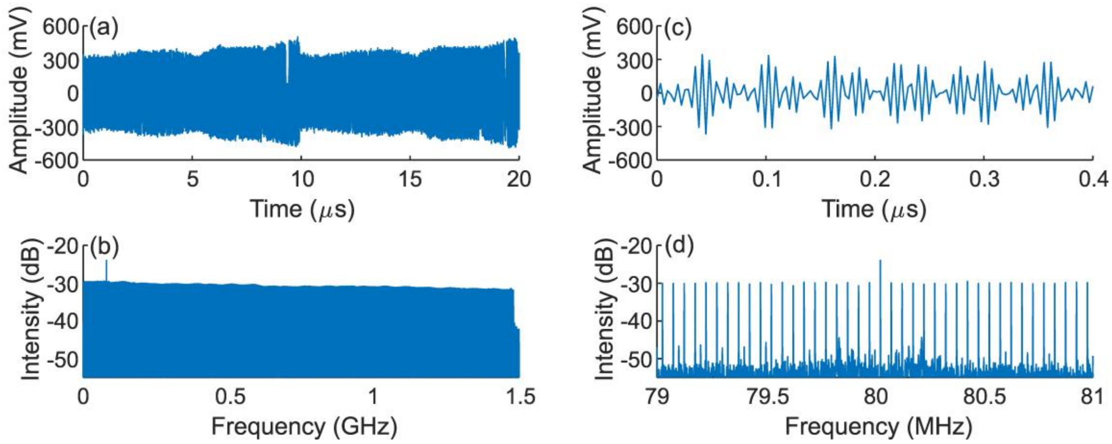

Figure S2 (a) Interferorgams and (b) radio frequency spectrum of the 100 kHz electro-optic frequency comb; (c) A zoom-in figure of (a); (d) A zoom-in figure of (b) in the region of AOM center shift.

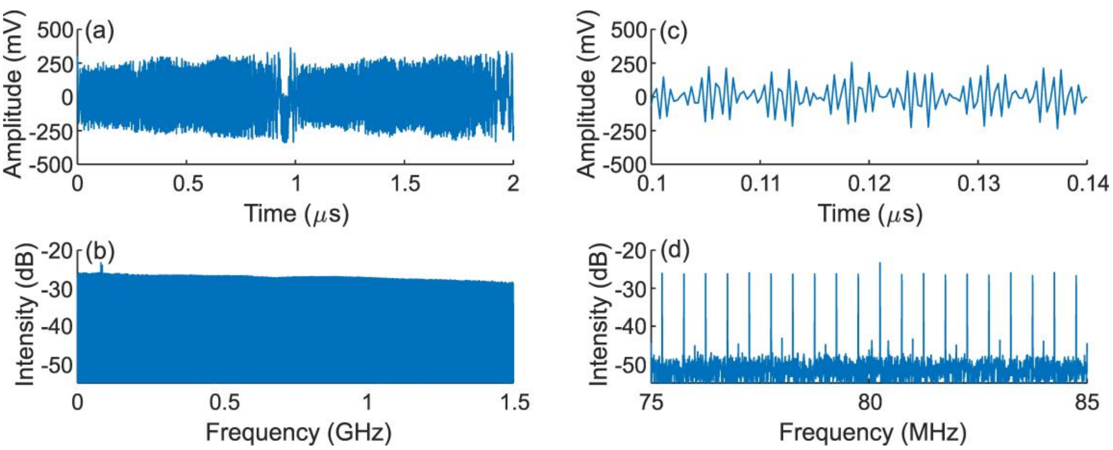

Figure S3 (a) Interferorgams and (b) radio frequency spectrum of the 1 MHz electro-optic frequency comb; (c) A zoom-in figure of (a); (d) A zoom-in figure of (b).

4. Simulation of cross-correlation linewidth of WGM speckle-based wavemeter

The wavelength of probe laser in the proposed scheme is determined by cross-correlation algorithm from the WGM speckle. The resolution depends on the linewidth of cross-correlation peak and its signal-to-noise ratio. Here, we explore how the Q-factor, the number of modes, and frequency range of WGM speckles affect the linewidth of cross-correlation peak and its noise level, on which the resolution may depend. Simulation analyses are performed based on the theory of WGM. Simulation analyses are performed using transfer matrix of micro-ring resonator based on the theory of WGM. Since WGM resonator support lots of modes, it can be approximately considered that the WGM resonator is formed by the superposition of multiple micro-rings in simulation. Each micro-ring is a WGM mode. The Q-factor and free spectral range (FSR) of each mode are slightly different, but on the same level. By adjusting the coupling coefficient and micro-ring radius, changes in Q-factor and FSR can be achieved. As shown in Fig. S4, simulated WGM speckles with Q-factor of 10^6 and 10^7 are generated with different coupling coefficient.

Firstly, we discussed the effect of Q-factor. As illustrated in Fig. S5, a cross-correlation peak with a narrower full width at half maximum (FWHM) and lower noise floor is achieved for the case of using a resonator with a higher Q-factor. A more precise determination of the cross-correlation peak location can be realized for better wavelength resolution with higher Q-factor resonator.

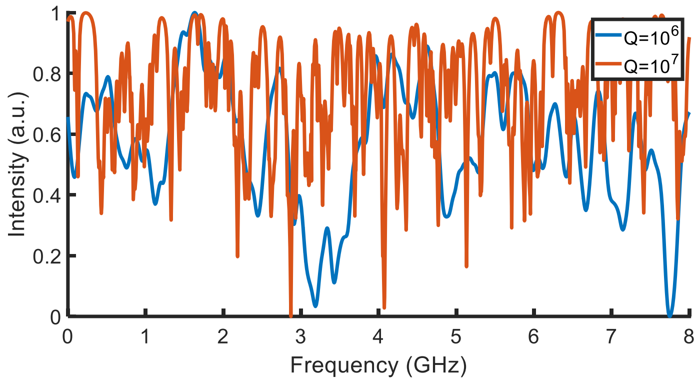

Figure S4 Simulated WGM speckles with Q-factor of 10^6 and 10^7, respectively.

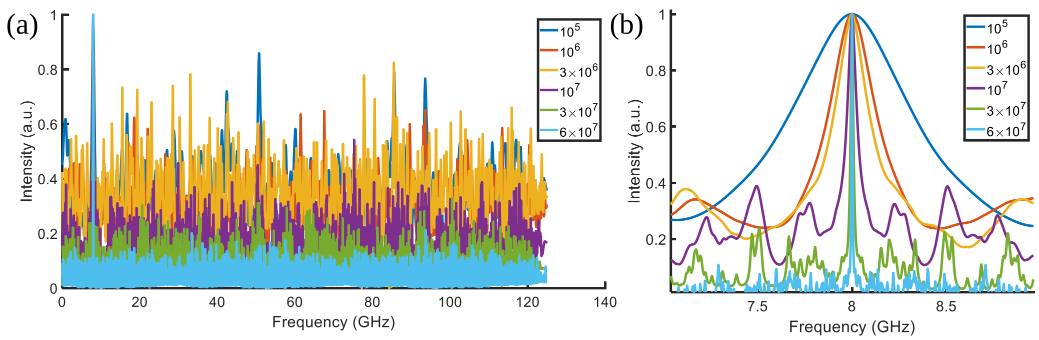

Figure S5 (a) Simulated cross-correlation results of WGM speckles with different Q-factors. The number of modes is 100. The frequency range of the measurement speckles is 8 GHz. (b) a zoom-in figure of (a) in the region of correlation peak.

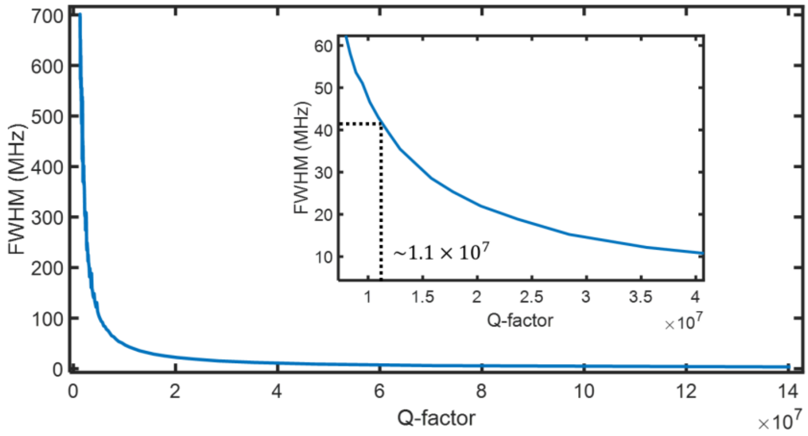

Figure S6 Simulation results of the relationship between Q-factor and FWHM of the correlation peak.

The relationship between Q-factor and the FWHM of the correlation peak in simulation is shown in Fig. S6. The simulation result shows that when Q-factor value reaches about 1.1×10^7, the corresponding FWHM is 41 MHz. In the experiment, the Q-factor of the fabricated resonator is about 10^7, and the FWHMs of the calculated cross-correlation peaks are about between 30 MHz to 50 MHz, which is consistent with the simulation results. Narrower FWHM means more precise determination of the cross-correlation peak location. Therefore, higher wavelength resolution can be achieved by WGM resonator with higher Q-factor.

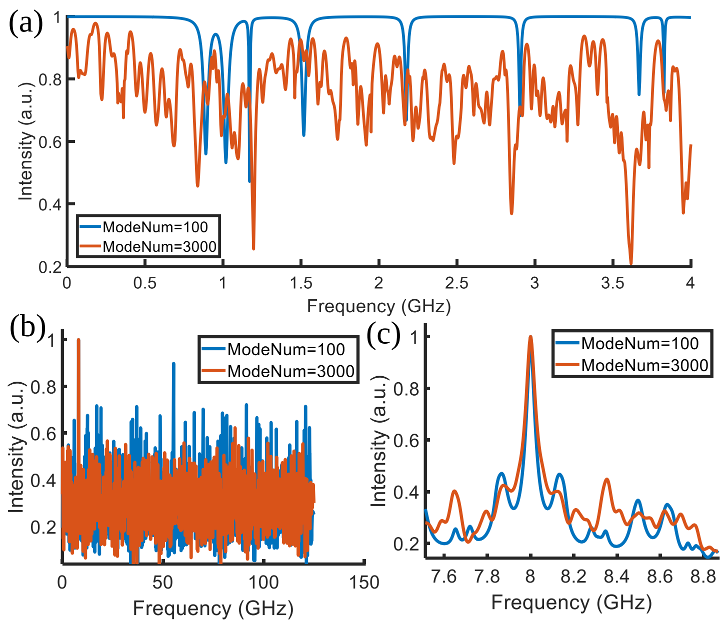

Figure S7 (a) The simulated WGM speckles with the mode number of 100 and 3000. The frequency range of the measurement speckles is 4 GHz. The Q-factor is 10^7. (b) Cross-correlation results between the measurement speckles in (a) and the corresponding reference speckles. (c) a zoom-in figure of (b) in the region of the correlation peak.

The effect of the number of modes for WGM speckle is depicted in Fig. S7(a). A larger number of modes produces more resonance peaks with same FWHMs in the speckle. Although the FWHM of the correlation peak is not reduced for the case of larger mode number, a fast measurement speed with a WGM speckle covering a smaller frequency range may be achieved. Besides, the correlation result with a smaller mode number suffers a lower signal-to-noise ratio as shown in Fig. S7(b) for the case of 100 modes.

The cross-correlation results of WGM speckles with different frequency ranges are shown in Fig. S8. Increasing frequency range has mild effect on the FWHM of correlation peak as shown in Fig. S8(d). Considering the reduction of noise level, the resolution may be improved with a larger frequency range.

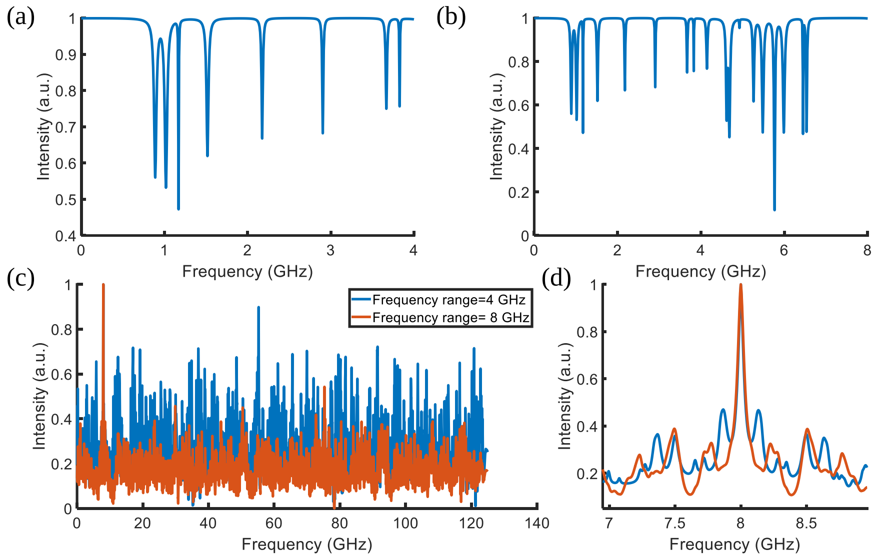

Figure S8 (a) The simulated WGM speckle covering a frequency range of 4 GHz. (b) The simulated WGM speckle covering a frequency range of 8 GHz. (c) Simulated cross-correlation results of WGM speckles with different frequency scanning ranges. The Q-factor is 10^7. The number of modes is 100. (d) a zoom-in figure of (c) in the region of correlation peak.

Calculation speed is important for real time measurement. When the sampling rate of speckle is 3.125 Gsa/s and the covering frequency range of reference speckle is 80 nm, the calculation time of cross-correlation is ~10 s at Matlab calculation platform with a CPU (i9-13900K). In future, computing speed can be accelerated by using more efficient computing resources and software platforms, such as FPGA and C++.

5. Additional data for simulation of Q-factor and free spectral range fluctuation

In order to quantitatively analyze the effects of Q factor and free spectral range, simulation is performed and results are shown in Fig. S9. As the Q-factor and FSR change, the WGM speckle gradually deforms until it is no longer correlated with the initial speckle pattern (cross-correlation coefficient lower than 0.5), as shown in Fig. S9 (b-e). To ensure the accuracy of reconstruction, the correlation coefficient between the distorted WGM speckle and the original WGM speckle should be larger than 0.5. The contour red line in Fig. S9 (a) illustrates the quantitative bound (Q factor is larger than 7.2×10^5, and free spectral range change is smaller than 12 kHz) maintaining a correlation coefficient above 0.5.

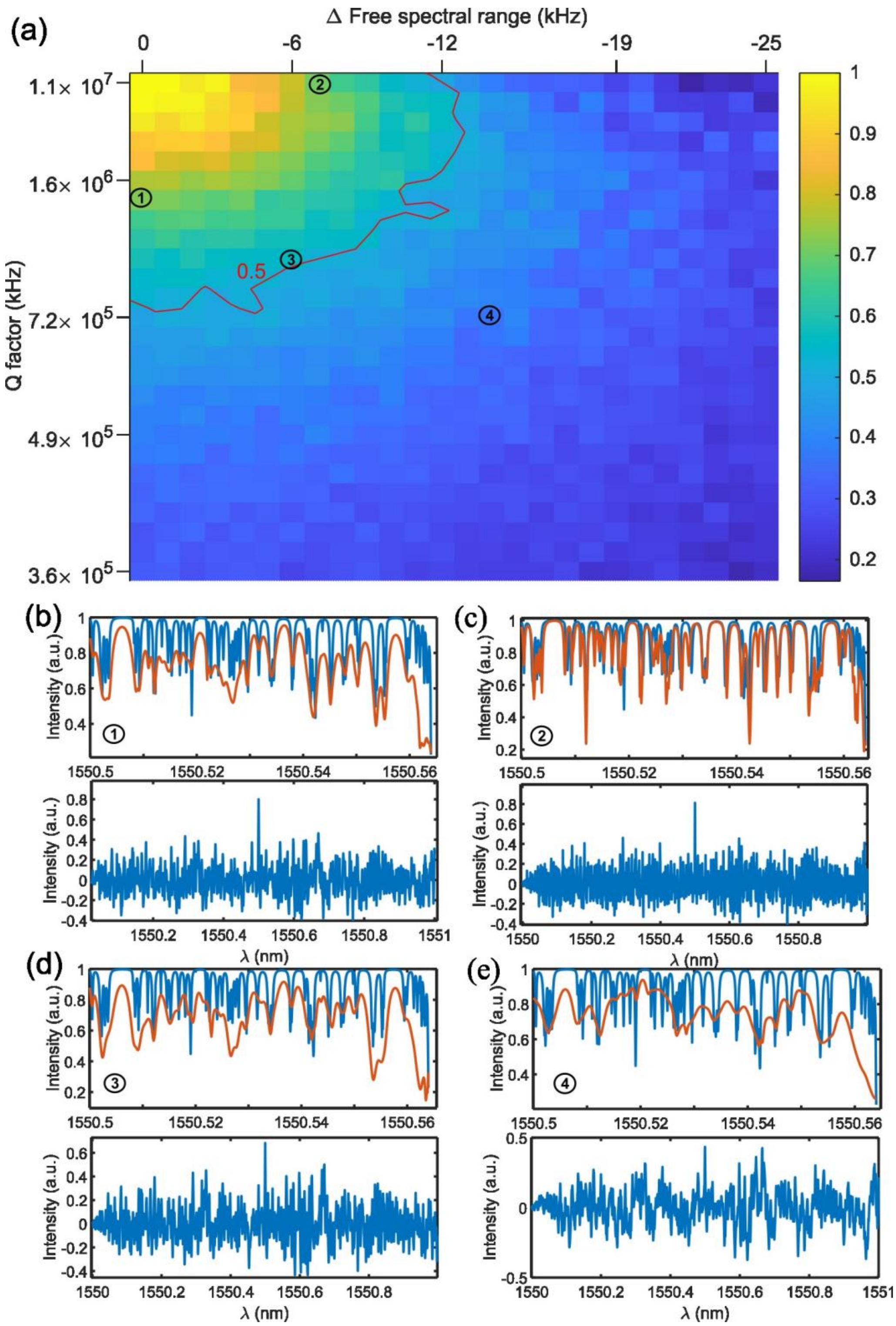

Figure S9 Simulation results. (a) Cross-correlation coefficient results between the distorted WGM speckle and the original WGM speckle with different Q-factor and FSR. (b) (c) (d) (e)

The distorted WGM speckle (in red) at mark 1, 2, 3, 4 in (a), and corresponding cross-correlation results. The original WGM speckle is in blue.